Sequential Robust Control Design Methodology Application to the MIMO Air Path of a Diesel Engine

Chao Deng, Guillaume Colin, Yann Chamaillard, Dominique Nelson Gruel

***Abstract*—This paper presents a methodology of robust control applied on a nonlinear MIMO system, on the air path of a turbocharged diesel engine. The methodology consists in first analyzing the MIMO system to observe dynamic properties with several tools, i.e. condition number, relative gain array and Gershgorin bands, before designing the controller. Hence, a sequential robust controller synthesis is proposed to obtain a decentralized control taking into account coupling and uncertainties of the nonlinear system. The results obtained from a Mean Value Engine Model (MVEM) engine simulation model show the real time applicability of the proposed method and the good control performances (good response time, no steady state error) for various engine speeds.**

***Index Terms*—Engine control, robust control, MIMO system, diesel engine, RGA and Gershgorin analysis**

I. INTRODUCTION

ENVIRONMENTAL and health issues have led to pollutant emission standards becoming more restrictive. Nowadays, a European diesel engine must emit less than 0.2g/km of Nitrogen Oxides (NO_X) and 0.005g/km of Particulate Matter (PM). In addition, CO_2 emissions and hence fuel consumption must be reduced in order to attain the goal set by the European Automobile Manufacturers' Association. As a result, the control task becomes more complex due to EGR and a small compliance window for air/fuel ratio. Research has therefore been focusing on achieving a trade-off between reducing pollutant emissions and fuel consumption while keeping the same performance. Turbocharged diesel engines are becoming increasingly attractive for passenger cars because of its better efficiency and power density, also because of their low fuel consumption and high torque at low speed.

In order to deal with diesel engine emission standards, the fuel path and air path (including Exhaust Gas Recirculation (EGR) and turbocharger) must be accurately controlled. This paper will focus especially on the air path. A certain number of studies, taking EGR, turbocharger and throttle into account on the air path of a diesel engine, can be found. For example, H infinity control was used to control the air path of a diesel engine [1], [2]. Another method, tested on the diesel engine, is inverse optimal control which gives a robust nonlinear control [3]. Ortner and del Re [4] proposed using new set points of data-based models to design a Model-based predictive controller (MPC) for diesel engines. Internal Model Control (IMC) can also be used to control a diesel engine. IMC and feedforward methods are combined together to obtain good control performance [5]. However, few works have dealt both with coupling and uncertainties of the process at the same time. This paper presents a methodology which considers the robustness, both the influence of uncertainties and coupling to a MIMO control system. Above all, it is relatively easy to tune and implement.

The idea is to extend a simply control design methodology to control a complex MIMO system, while considering the coupling and uncertainties with good robustness and performance, here it is PID pole placement control . Ahead of processing the control methodology, the properties of the MIMO system need to be analyzed. Consequently, a MIMO process coupling characters analysis and a Robust Sequential Multi-SISO control method are presented to against the uncertainties and coupling.

The paper is organized as follows. The air path model is presented in Section II. This system is analyzed in Section III; the results of the analysis suggest a means of controlling the MIMO system. The Robust Sequential Multi-SISO control method is therefore chosen in Section IV. In section V, simulation results are shown. Conclusions are made in the last section.

II. SYSTEM DESCRIPTION AND IDENTIFICATION

The system considered, shown in Fig. 1, is described as follows. Fresh air (Air flow Q_{air}) is aspirated into the compressor and cooled down by the intercooler. It then passes through the throttle into the intake manifold (pressure p_{man}) and then enters the cylinders to react with fuel. After exiting the cylinders, exhaust gases are collected by the exhaust manifold. The exhaust flow is then split into three parts: one returns to the intake manifold through an intercooler and an EGR Valve (V_{EGR}); another part is used to power up the turbine; and the last part is directly exhausted through the Wastegate Valve (V_{WG}). The dynamic coupling process is therefore a three-input-two-output air-path system. Due to the throttle always full opened during almost cases, this system is treated as two-input-two-output (with the throttle fully open for modeling the data, for system identification and the simulations). Therefore, the manipulated variables are V_{EGR} and V_{WG}, and the two controlled variables are Q_{air} and p_{man}.

Since V_{EGR} (respectively V_{WG}) and Q_{air} (resp. p_{man}) are strongly related, a decentralized control can be envisaged. Nevertheless, coupling cannot be neglected [6].

This project is co-financed by the European Union: Europe is committed to the region Centre with the European Regional Development Fund.
Manuscript has been received May 10, 2012

Chao. Deng, Guillaume. Colin, Yann. Chamaillard, are with Laboratory PRISME, EA4229 University of Orléans, 8, rue Léonard de Vinci, 45072 Orléans, France (chao.deng@etu.univ-orleans.fr).

Dominique. Nelson Gruel is with University of Bordeaux, IPB, IMS CNRS UMR5218 France

The principle of this global control scheme is as follows: first, the driver fixes the position of the pedal, which is translated into a torque set point by a supervisor; generally, the torque set point is translated into a fuel mass set point by look-up tables, as a function of engine speed. Next, air mass flow reference points (Q_{airref}) and intake manifold pressure reference points (p_{manref}) are deduced. V_{EGR} and V_{WG} are then adjusted by the controller.

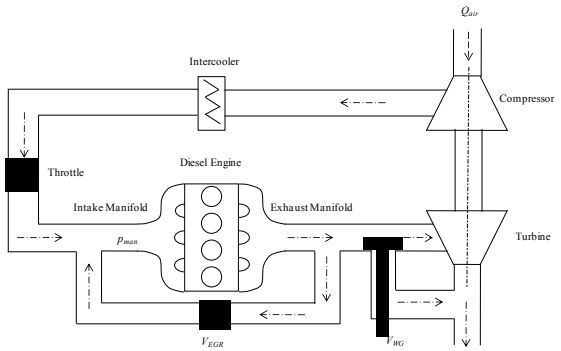

Fig. 1. Air path of a turbocharged diesel engine

The control scheme is shown in Fig. 3.

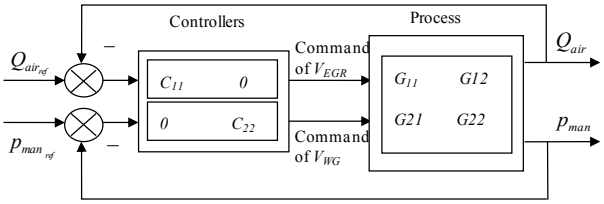

Fig. 2. Global control scheme for the air path of a diesel engine

The engine considered here is a PSA DW10ATED, which is a 2.0L turbocharged 4-cylinder diesel engine with direct injection. All the air path actuators are pneumatic (wastegate, EGR and throttle). The Mean Value Engine Model (MVEM) simulation model used here was calibrated on our engine test bench [7].

In this section, system identification is split into two parts. First, the input/output signals are normalized to facilitate the comparison of variables. Second, a Fourier Transform is used to obtain frequency data.

A. Normalization, linearization and de-normalization

In order to analyze the system easily, the input and output variables are normalized and linearized, the normalized variable values are small and close to zero. Depending on the system normalization, blocks of normalization and de-normalization must be added to the system as shown in Fig 2[8].

De-normalization of the input is computed with (1), and normalization of the output with (2) [6].

$$v = v_m(\delta v + 1) \tag{1}$$

$$\delta w = \frac{w}{w_m} - 1 \tag{2}$$

where δv is the normalized input signal, v is the system input, v_m is the average value of v, w is the output, w_m is the average value of w, and δw is the normalized output signal. The system is derived by the experiment data.

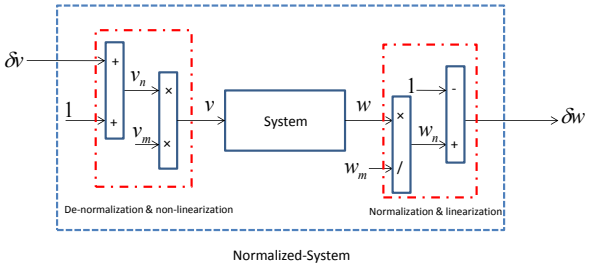

Fig. 3. Scheme of the normalized system

B. Frequency identification

Here, 54 operating points (torque versus engine speed) were chosen for system identification. The engine speed ranged from 1000 rpm to 4000 rpm and the torque from 25 Nm to 125 Nm. In order to describe the system on all operating points, in the frequency domain, a Fast Fourier Transform is performed, giving the Bode diagrams shown in Fig. 4,

- G_{11} is from V_{EGR} (in %) to Q_{air} (in g/s).
- G_{12} is from V_{WG} (in %) to Q_{air} (in g/s).
- G_{21} is from V_{EGR} (in %) to p_{man} (in bar).
- G_{22} is from V_{WG} (in %) to p_{man} (in bar).

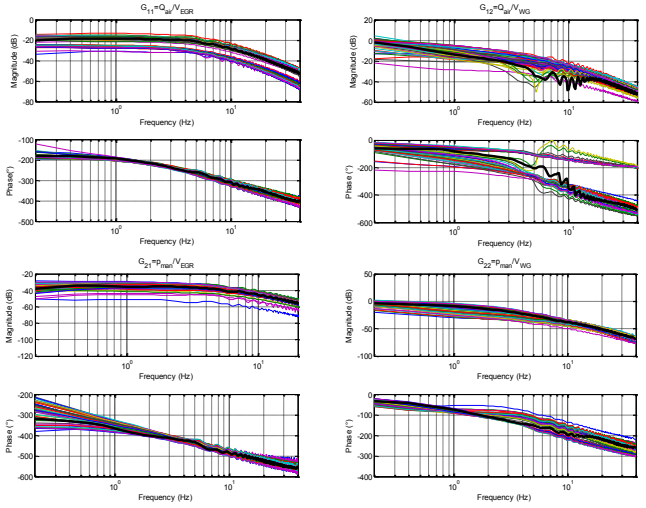

Fig. 4. Bode diagrams of the process $G(j\omega)=\begin{bmatrix} G_{11} & G_{12} \\ G_{21} & G_{22} \end{bmatrix}$ (thick black solid curves are nominal plants, and the other curves are plants on 54 operating points)

The nominal process, shown in Fig 4 by a thick solid line, is chosen as :

$$G(j\omega)_{\text{nominal}} = \frac{\overline{G(j\omega)} + \underline{G(j\omega)}}{2}, \forall \omega \tag{3}$$

where $G(j\omega)_{nominal}$ is the nominal process, $\overline{G(j\omega)}$ (resp. $\underline{G(j\omega)}$) is the maximum (resp. minimum) of all processes at each frequency. One can note that this nominal process, corresponding to the center of the uncertainties and used for the control synthesis, has no physical meaning.

Simple linear models are finally obtained by minimizing the sum of square errors with the system identification

toolbox of Matlab®. A second order model represents well the nominal diagonal process of $G(j\omega)_{nominal}$ on the Fig. 5.

$$N_{ii}(s) = \begin{cases} \dfrac{-0.13}{(0.027s+1)^2} & \text{if } i = 1 \\ \dfrac{0.74}{(0.29s+1)(0.05s+1)} & \text{if } i = 2 \end{cases} \quad (4)$$

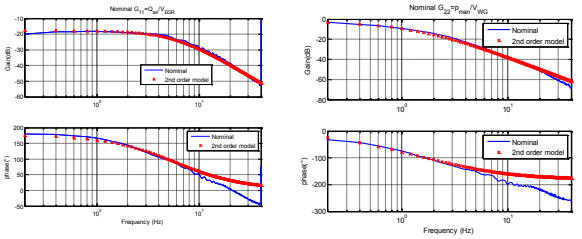

Fig. 5. Bode diagram of the nominal model $N_{ii}(s)$ and of the nominal process $G(j\omega)$ on their diagonals

III. MIMO SYSTEM ANALYSIS

Because of the priori necessary of the system, Condition numbers (CN), Relative Gain Array (RGA), and Gershgorin Bands (GB) are used for the coupling and uncertainties, the degree of sensitivity and intersection, the pairing of input and output channels and the deduction of control design method.

A. Condition Number (CN)

Condition number is a way to quantify the degree of directionality and is rigorously related to system error sensitivity and robustness but it is scale dependent [8]. A large condition number indicates sensitivity to input unstructured uncertainty.

The condition number $\gamma(G)$ is defined by

$$\gamma(G) = \overline{\sigma}(G) / \underline{\sigma}(G) \quad (5)$$

where $\overline{\sigma}$ (resp. $\underline{\sigma}$) is maximum (resp. minimum) of singular value(SV), which is defined as follows,

$$\sigma(G(j\omega)) = \sqrt{\lambda(G(j\omega)^H \cdot G(j\omega))} \quad (6)$$

where σ is SV, $G(j\omega)^H$ is the complex conjugate transpose of the process and λ is the eigenvalue.

As CN is scale dependent, two scales are compared in Fig. 4, namely the normalized system (from δv to δw) and the non-normalized system (from v to w) (see section II. A).

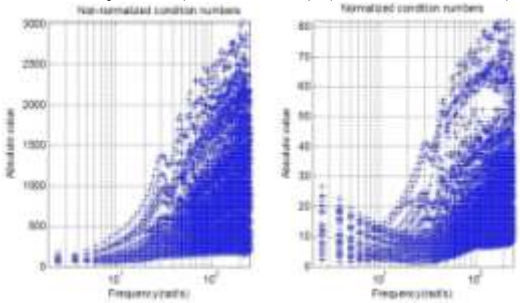

Fig. 6. Comparison of condition numbers on 54 operating points from 2 rad/s to 250 rad/s

From Fig. 6, it can be seen that if the system is normalized, CN is decreased from 3000 to less than 82. Hence, normalization enables the condition numbers to be reduced on all operating points. In both cases, the system is more sensitive at high frequencies but within acceptable limits, because of the useful frequencies (ω_c) considered. ω_c is derived by the sensitivity function of the closed-loop according to the specifications of system, thus ω_c for the first loop is 13.2 rad/s and for the second loop is 2 rad/s. For the whole system, ω_c is chosen the bigger one from the two useful frequencies.

Therefore, if the system is ill-conditioned, normalization is a way of decreasing sensitivity to unstructured input uncertainty. Furthermore, it is valuable to note that optimal condition number (OCN) can be used to minimize the condition number value [9].

B. Relative Gain Array (RGA)

RGA is an indicator of sensitivity to uncertainty for a coupled system. It measures the degree of interaction or decoupling, in order to detect the potential difficulty of achieving robustness considering a diagonal multiplicative uncertainty at the plant input [9]. It provides a way of finding the desired pairing between controlled variables and manipulated variables. The RGA, which is scale independent [9], is defined for a square system below.

The RGA of a nonsingular complex matrix G is a square complex matrix, which is defined as [9]:

$$\Lambda(G(j\omega)) = G(j\omega) \times (G(j\omega)^{-1})^T \quad (7)$$

where $G(j\omega)$ is a MIMO system at frequency ω, and × represents element-by-element multiplication (Schur product).

RGA is shown from 2 rad/s to 250 rad/s in Fig. 7.

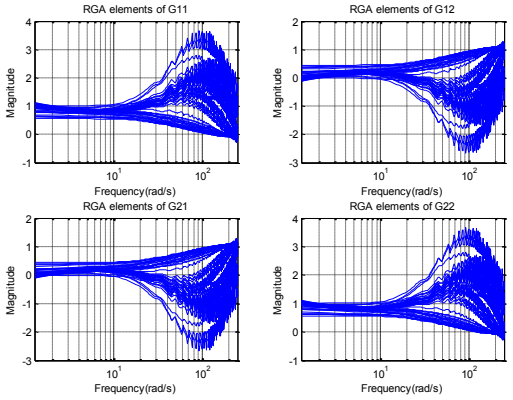

Fig. 7. Real part of the RGA elements on 54 operating points (2 rad/s to 250rad/s)

Fig. 7 shows that they are not large RGA-elements. In the range of ω_c, the values of RGA for G_{11} and G_{22} are closer to 1 than G_{12} and G_{21}. Moreover as off-diagonal RGA-elements having negative values they should be avoided to pair input and output. Hence, G_{11} and G_{22} should be chosen as the main plants. Before ω_C (13.2 rad/s), RGA-elements are smaller than 1.2 (in fact close to unity matrix), which implies a major link from input to output on the diagonal. The manipulated variable V_{EGR} (resp. V_{WG}) therefore affects the output Q_{air} (resp. p_{man}) more directly.

The analysis of RGA shows that the input V_{EGR} is strongly

coupled with Q_{air} and that V_{WG} is strongly coupled with p_{man}. A decentralized controller therefore is used.

However, with CN and RGA, it is still impossible to find the details of coupling of loop 1 and loop 2 in this 2X2 system. Fortunately, Gershgorin bands are considered to take these details into account. Above all, they provide a useful theoretical basis for the stability analysis of dominant systems [10].

C. Gershgorin Bands (GB)

For a MIMO system, the Gershgorin bands theory is a way to determine the coupling grade and the stability. If the Gershgorin bands are thin and exclude the critical point -1, the system *G(s)* is diagonally dominant and stable. Hence it is considered as a decoupled system and so a decentralized controller will be sufficient [11].

Gershgorin Bands: On the Nyquist diagram of $g_{i,i}(s)$, on each point a circle with a radius of $\min(\sum_{i=1,i\neq j}^{m}|g_{i,j}(s)|, \sum_{i=1,i\neq j}^{m}|g_{i,j}(s)|)$ is super imposed, which corresponds to the effect of the non-diagonal elements. The bands obtained in this way are called Gershgorin Bands [10].

The bands and diagonally dominant elements are plotted in Fig. 8.

From the left-hand plot in Fig. 8, it can be seen that in loop 1, G_{11} has thin bands and excludes the critical point, and that the disturbance of loop 1 is small; this loop is therefore highly decoupled and stable.

The right-hand plot in Fig. 8 shows that in loop 2, G_{22} has very thick bands and for one operating point includes the critical point. Therefore, loop 2 is coupled with G_{12}, when considering a decentralized controller, coupling must be taken into account for synthesis.

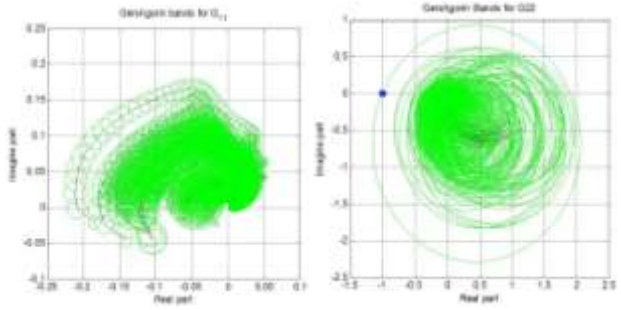

Fig. 8. The Gershgorin Bands in 54 operating points (On the left: GB for loop 1; on the right: GB for loop 2; center curves are G_{11} and G_{22}, circles are the disturbances of G_{21} and G_{12})

However, the stability conditions are only sufficient but not necessary [11], hence it cannot be concluded that this loop is unstable.

In view of the thin bands for loop1, a decentralized controller and coupling are considered through Gershgorin bands. For Loop 2 a decentralized controller is also considered, but because of the thick bands, coupling must be explicitly taken into account for synthesis, is discussed in the following section.

D. System analysis conclusion

As shown by CN, our system without normalization seems to be ill-conditioned, therefore it is sensitive to unstructured input uncertainty. A very important result is that the normalization step reduces the CN.

RGA analysis has shown that the input V_{EGR} is strongly coupled with Q_{air} , and V_{WG} is strongly coupled with p_{man}. A decentralized controller therefore is used.

Applying Gershgorin Band theory for loop 1 a decentralized controller will be synthesized (coupling through Gershgorin bands), and for loop 2 the controller will be synthesized taking the overall system and the first closed loop into account.

This two-step process is called a sequential robust controller synthesis, which considers the coupling and uncertainties to ensure the robust stability.

IV. MIMO CONTROL SYSTEM DESIGN AND SYNTHESIS

A. Specifications

Reasonable desired performances have been fixed as a function of the system dynamics and physical properties.

For Q_{air} and p_{man} respectively, the overshoots were set at 5% and 3%, and the response times at 0.3s and 1.5s (the sensitivity function bandwidths were 13.2 rad/s and 2 rad/s).

B. Sequential Multi-SISO Control design

Regarding the results of the analysis of the MIMO system properties, a sequential robust multi-SISO method is proposed to control this MIMO system. In this article, considering the transfer function (4), a second order system pole placement design is used [11].The open loop system and controller are:

$$N_{ii}(s) = \frac{K_p}{(1+sT_1)(1+sT_2)} \tag{8}$$

$$C(s) = \frac{K(1+sT_i+s^2T_iT_d)}{sT_i} \tag{9}$$

$$T(s) = \frac{C(s)N_{ii}(s)}{1+C(s)N_{ii}(s)} \tag{10}$$

where $N_{ii}(s)$ is the original plant, *Kp* is the open-loop gain of the plant, T_1 and T_2 are time constants, *C(s)* is a PID controller, *K*, T_i, T_d are the tuning parameters of *C(s)*, and *T(s)* is the equivalent closed loop transfer function. In order to find the controller, a desired third order system *R(s)* is defined as:

$$R(s) = \frac{\alpha\omega_n^{\ 3}}{(s+\alpha\omega_n)(s^2+2\zeta\omega_n s+\omega_n^{\ 2})} \tag{11}$$

where ω_n is the desired natural frequency, and ζ is the desired damping ratio.

a. Control design for Loop 1

As demonstrated by CN and RGA analysis, the pole placement method is used directly on $N_{11}(s)$ to find the PID controller parameters for loop 1. Using the given

specifications, the controller parameters are found to be K=-26.5726, T_i=0.0564 and T_d=0.0332.

b. Control design for Loop 2

As shown CN and RGA analysis G_{22} has coupling with G_{12} (G_{22} is not diagonally dominant); an equivalent plant G_{22}*(s) must therefore be used [12].This equivalent plant is defined as a function of the first controller $C_1(s)$ on all plants:

$$G_{22}^{*}(s) = G_{22}(s) - \frac{G_{21}(s)C_{11}(s)G_{12}(s)}{1+C_{11}(s)G_{11}(s)} \qquad (12)$$

The equivalent nominal model is also deduced:

$$N_{22}^{*}(s) = \frac{0.89}{(0.2s+1)(0.06s+1)} \qquad (13)$$

The pole placement method can be used on N_{22}*(s) to find the controller parameters for loop 2. Taking the specifications for loop 2, the controller parameters are deduced, namely K=2.1780, T_i =0.2669, and T_d =0.1451.

C. Robust Stability

C.1 Uncertainty modeling

To propose a robust approach for the controller, the uncertainties first need to be described [8]. On non-parametric uncertainties, assuming that the system is described by a nominal transfer function $G(j\omega)$, then the associated uncertainty is modeled using an uncertainty bound described by a transfer function $W(j\omega)$ [7]. Here a multiplicative uncertainty description is used, where the set S is defined:

$$S = \left\{ G(j\omega)(1+\Delta W(j\omega)) \middle\| \|\Delta\| \le 1, \arg\{\Delta\} \in [-\pi, \pi] \right\} \qquad (14)$$

where Δ is the uncertainty generator which has no physical meaning.

To find the suitable $W(j\omega)$ for this system, the maximum distance $W(j\omega)^{\dagger}$ between the nominal plant N and all the processes for each frequency must also be computed:

$$W(j\omega)^{\dagger} = \max\left(\frac{|N(j\omega) - G(j\omega)|}{|N(j\omega)|} \right) \forall \omega \qquad (15)$$

$W(j\omega)^{\dagger}$ is point to point frequency description. The transfer function $W(j\omega)$ for uncertainty bound modeling is also deduced as the best equivalent approximation of $W(j\omega)^{\dagger}$. Respectively for G_{11} and G_{22}*, $W(j\omega)$ are:

$$W_{11} = \frac{0.02\,\mathrm{s} + 0.82}{0.015\mathrm{s} + 1} \qquad W_{22} = \frac{0.08s+1}{0.04s+1} \qquad (16)$$

Fig. 9 shows the Gershgorin band for loop 1 and uncertainty bounds $W(j\omega)$ of loop 1 and loop 2. The coupling disturbances of Loop 1 (Gershgorin bands) are covered by the overall uncertainty. Hence, in this case, for loop 1, all the uncertainties and disturbances are well described by the uncertainty bound $W_{11}(j\omega)$. For loop 2, since G_{22}* takes into account the overall system with the first closed loop, $W_{22}(j\omega)$ also describes uncertainties and disturbances well.

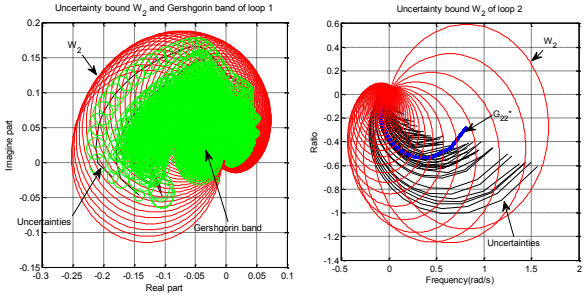

Fig. 9. Gershgorin band for loop 1 (left) and uncertainty bounds $W(s)$ of loop 1 (left) and loop 2 (right)

C.2 Stability check

The stability robustness can be checked with the Nyquist stability theorem.

$$|L(s)\cdot W(s)| < |1 + L(s)| \qquad (17)$$

where $L(s)$ is the loop gain, and $L(s)= G(s)\cdot C(s)$. The bounds of two loops are plotted Fig. 10.

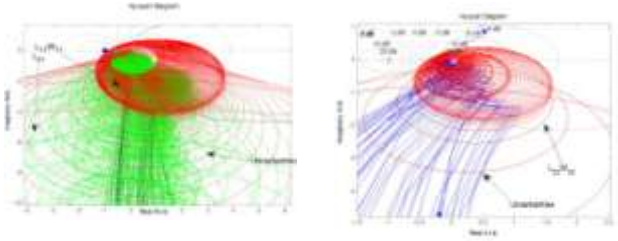

Fig. 10. Nyquist stability proof for Loop 1 (left) and Loop 2(right). $L_{11}W_{11}$, $L_{22}W_{22}$ are loop gains of uncertainties, L_{21} is the Gershgorin disturbance band of loop 1.

In Fig. 10 it can be seen that in both cases the critical point is never encircled ($\boldsymbol{L_{11}W_{11}}$, $\boldsymbol{L_{22}W_{22}}$).

We concluded that these two loops have stability robustness, in terms of both uncertainties and disturbances.

Moreover, it is necessary to mention that the stability margins in terms of maximum sensitivity amplitude and the uncertainty bands and Gershgorin bands, which is the minimum value of ($|1+L(j\omega)|$- $|L(j\omega)W(j\omega)|$). Hence, the stability margin is 0.317 for the first loop (resp. 0.4491 for the second loop).

V. Simulation Results

The simulation model is a nonlinear model based on physical equations (e.g. thermodynamic principles for volumes, Barré de St Venant equations for restrictions…) and on look-up tables (e.g. volumetric efficiency, turbocharger…) [13].All the simulation results shown here were performed with LMS/AMESim. The Robust Sequential Multi-SISO control design was checked in various test scenarios.

All the results presented here were obtained with the two controllers defined in section *IV. B*. Considering static saturations of the actuators (V_{EGR} and V_{WG}) in a real engine, a classical anti-reset windup was added [12] . The time constant T_t of anti-windup was fixed at T_t= T_i /2. The analysis of stability of the system with anti-reset windup can be carried out using small-gain arguments, and linear norm-bounded uncertainties in the plant model can be incorporated

by augmenting the block Δ shown above equation (14) with linear blocks [14].

The simulated scenario for the engine's torque is varied at each four seconds, and its values are from 25Nm to 125Nm by scenario simulations in a period of 24 seconds.

The limit for V_{EGR} goes from 0% to a maximum openness limit which depends on the engine speed, and the limit for V_{WG} goes from 40% to 80% of closeness limit. The dynamic of the actuators of EGR and WG valves are modeled by the step signals. The controller has been validated on different transients at two engine speeds (1500 rpm and 2500 rpm) as shown in Figs. 11 and 12, which shows the control results for the two different engine speeds considered. We see the good behavior and robustness of the control results for both loops (Q_{air} and p_{man}) according to the specifications.

As expected, the closed loop system is stable without oscillation and steady state error. Concerning dynamic performance, it appears that the closed loop behavior is robust with regard to engine speed and torque variations. Due to the approach (only one controller synthesis for one nominal system) the dynamic behavior is not constant but nonetheless remains highly acceptable. It is worth noting that this is due to the normalization (and de-normalization) step, which creates an implicit feedforward and gain scheduling into the control scheme.

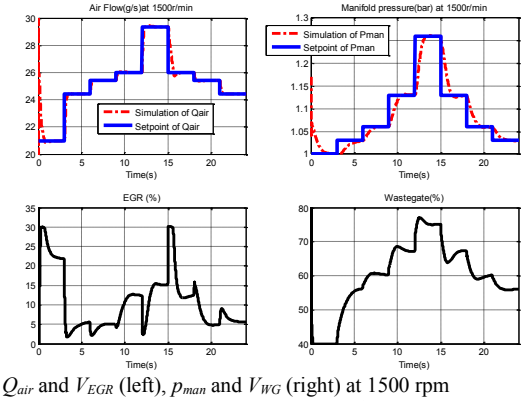

Fig. 11. Q_{air} and V_{EGR} (left), p_{man} and V_{WG} (right) at 1500 rpm

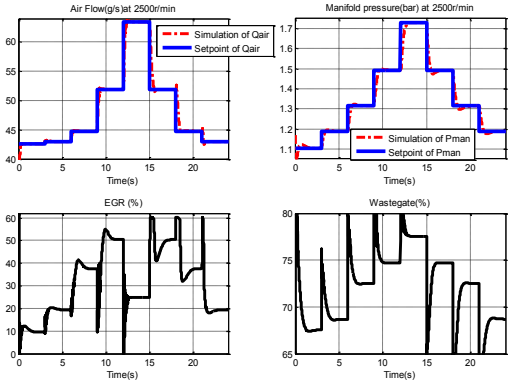

Fig. 12. Q_{air} and V_{EGR} (left), p_{man} and V_{WG} (right) at 2500 rpm

In addition, as it can be seen in Fig. 11 (between 15s and 16s V_{EGR} saturates at 30%), the actuator saturation effects are well mastered thanks to the anti reset windup.

All in all, the results show that the control design meets our robustness control design requirements, thus validating the performance.

VI. Conclusions

The paper has first proposed an in-depth analysis of the structural properties of nonlinear MIMO systems. The RGA and Gershgorin Bands analysis yield good MIMO system properties: with regard to uncertainty and coupling it is shown that a sequential decentralized MIMO robust control is efficiently used.

The CN analysis shows that the normalization step reduces conditioning, thereby reducing unstructured input uncertainty sensitivity. In this way, a PID controller - in spite of its simplicity -, synthesized by pole placement, gives good results which meet the specifications. A further advantage is that a linear PID controller is real time applicable.

The proposed method has been illustrated and validated on the control of the air path of a diesel engine in a highly representative simulator.

References

[1] X. K. Wei, L. del Re, 2007. Gain scheduled H∞ control for air path systems of diesel engines using LPV techniques. IEEE transactions on control systems technology, 15(3):406-415.

[2] M. Lee, M. Sunwoo, 2012. Modelling and H∞ control of diesel engine boost pressure using a linear parameter varying technique. Journal of Automobile Engineering. vol. 226 no. 2 210-224

[3] J. Wahlstrom , L. Eriksson, 2008. Robust Nonlinear EGR and VGT Control with Integral Action for Diesel Engines. Proceedings of the 17th World Congress, Seoul, Korea, p.2057-2062

[4] P. Ortner, del L. Re, 2007. Predictive control of a diesel engine air path, IEEE transactions on control systems technology, 15(3): 449-456.

[5] R. Nitsche, J. Hanschke, D. Schwarzmann, 2006. Nonlinear internal model control of diesel air systems. E-COSM-Rencontres Scientifiques de l'IFP Proceeding, p.121-131.

[6] G. Colin, Y. Chamaillard, B. Bellicaud, 2011a. Robust Control for adownsized SI engine. Proceeding of the iMeche, Journal of Automobile Engineering. [doi: 10.1177/0954407011401503]

[7] B. Jonas, 2004. Mean Value Engine Model of a heavy duty diesel engine. ISRN: LITH-ISY-R62666.

[8] L. Guzzella, 2007. *Analysis and synthesis of Single-input Single-output control systems*. Verlag der Fachvereine Hochschulverlag AG an der ETH Zurich, ETH Zurich.

[9] S. Skogestad, I. Postlethwaite, 2005. *Multivariable feedback control Analysis and design*. Wiley-Interscience,

[10] D. Garcia, A. Karimi, R. Longchamp, 2005. PID Controller design for multivariable systems using gershgorin bands. IFAC World Congress. 16(1): Czech Republic.

[11] J. Mikleš, M. Fikar, 2007. *Process Modelling, Identification, and Control*. Springer, Erich Kirchner, Heidelberg, p.272-273

[12] G. Colin, P. Lanusse, A. Louzimi, Chamaillard, Y., Deng C., Nelson-Gruel, D., 2011b. Multi-SISO Robust Design for the Air Path Control of a Diesel Engine. IFAC World Congress. Milan.

[13] Guzzella, L. and Onder C., 2004. *Introduction to Modeling and Control of Internal Combustion Engine Systems*. Springer.

[14] Kothare, M. V., Campo, P.J., Morari, M., Nett. C.N., 1993. A Unified Framework for the Study of Anti-Windup Designs. Chemical Engineering. p.24-26